

A simple method for the kinetic quantification of carbocysteine in drug formulations

Abhishek SRIVASTAVA ^{1*}, Ruchi SINGH ², Neetu SRIVASTAVA ³, Manjusha DIWAN ⁴

¹ Department of Chemistry, GLA University, Mathura, 281006, U.P., India

² Department of Chemistry, B. N College of Engineering & Technology, Lucknow, U.P., India

³ Department of Chemistry, DDU Gorakhpur University, Gorakhpur, 273001, UP (India)

⁴ Bio-Analytical Division, Shriram Institute for Industrial Research, 19-University Road, 110007-Delhi, India

* Corresponding Author. E-mail: aabhi@chem.gla.ac.in (A.S.); Tel. +91-962-796 90 85.

Received: 19 October 2022 / Revised: 05 December 2022 / Accepted: 05 December 2022

ABSTRACT: A simple, reproducible, and rapid kinetic method for the S-Carboxymethyl-L-cysteine (CCys) determination has been proposed and linked to CCys quantification in pharmaceutical preparations. The method is based on the inhibitory feature of Carbocysteine. CCys forms a stable complex with Hg^{2+} and reduces the actual Hg^{2+} concentration and ultimately the rate of reaction between pyrazine (Pz) and $[Ru(CN)_6]^{4-}$ catalyzed by Hg^{2+} . Under the optimized reaction conditions with ionic strength (I) = 0.1 mol dm⁻³ (KCl), [Pyrazine (Pz)] = 3.0×10^{-4} mol dm⁻³, pH = 4.0 \pm 0.03, $[Hg^{2+}] = 1.5 \times 10^{-4}$ mol dm⁻³, $[Ru(CN)_6]^{4-} = 2.75 \times 10^{-5}$ mol dm⁻³, and at 45.0 \pm 0.2 °C temperature, fixed time of 9 and 14 min was selected to compute the absorbance at 370 nm corresponding to the ultimate reaction product $[Fe(CN)_5Pz]^{3-}$. With the proposed kinetic spectrophotometric method, the micro-level quantification of CCys in distinct water samples can be done down to 1.25×10^{-6} mol dm⁻³. The developed procedure is highly reproducible and can be efficiently used to quantitatively estimate the CCys in the drug samples with high accuracy. The general additives present in drugs do not substantially interfere in the determination of CCys even up to 1000 times with [CCys].

KEYWORDS: Hexacyanoruthenate(II); Excipients; Catalyst inhibitor complex; Ligand substitution reaction; Inhibitory effect, Carbocysteine.

1. INTRODUCTION

A mucolytic drug carbocysteine (CCys) is used for the treatment of respiratory tract disorders by reducing the viscosity of the mucus in the windpipe, nose and lungs by cleaving the disulfide linkage between the mucin monomers.^[1, 2] People suffering from chronic obstructive pulmonary disorder (COPD) and bronchiectasis are medicated with carbocysteine for the easy expulsion of mucus.^[3] Carbocysteine also exhibits anti-inflammatory and anti-oxidative properties.^[4, 5] Its side effects include gastrointestinal bleeding, dizziness, headache, and skin rashes.^[6, 7] It is a thioether of tri-functional amino acid L-cysteine (containing thiol, amino, and carboxylic groups) in which carboxymethyl group has replaced one hydrogen of thiol. Figure 1 represents the structure of carbocysteine.

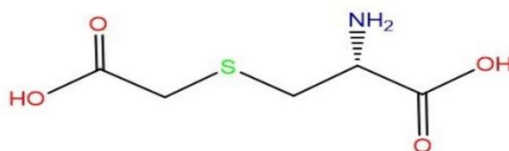


Figure 1: Structure of Carbocysteine

For centuries, sulfur continues to be the dominating heteroatom in the wide varieties of FDA-approved drugs and bioactive molecules. Organosulfur compounds play a specific role in the distinct

How to cite this article: Srivastava A, Singh R, Srivastava N, Diwan M. A simple method for the kinetic quantification of carbocysteine in drug formulations. J Res Pharm. 2023; 27(1): 299-310.

metabolic process as enzyme and structural proteins. [8-11] The pharmaceutical industry is always looking towards analytical chemists for the efficient methodology for the detection and quantification of sulfur-bearing bioactive molecules and drugs in distinct samples. The fundamental importance and immediate applications of redox/ligand exchange reactions of transition metal complexes in synthetic, analytical, and organometallic chemistry attracted many chemists for their kinetic study. [12-17] Numerous kinetic reports on oxidation of Fe(II)/Co(II) complexes and cyanide substitution from cyano complexes of Fe(II)/Ru(II) are available in literature. [18-19]

Different approaches for the quantification of thio compounds in biological, analytical and drug samples are oftenly used. [20-22] The quantification methodology includes voltammetry, [23] flow injection analysis, [24] NMR-spectrometry, [25] fluorimetry, [26] colorimetry, [20] chromatography, [27-29] spectrophotometry, [30,31], electrochemical, [32] and potentiometry. [33] Table 1 describes the various analytical methods used for the determination of sulfur bearing drugs/compounds with their detection limit. The main drawbacks of above-mentioned methods may include high initial investment, time-consuming process, heavy instrumentation, and high cost for sample analysis. Very few reports are available on kinetic spectrophotometric method, which require only UV-Visible spectrophotometer for drug quantification. [34-36]

Table 1. Analytical methods used for quantification of sulfur containing drugs

Method	Description	Detection Limit	Reference
Voltammetry	Platinum electrode was used as working electrode	50 μ M	23
Fluorimetric method	The proposed method based on the reaction of carbocysteine with roth's reagent	5 ng/mL	26
Ion exchange Chromatography	Carbocysteine determination in pharmaceuticals is based on non-suppressed conductimetric detection	0.14 μ g/ml	27
LC-MS/MS	Carbocysteine in human plasma was determined by protein precipitation extraction method	50-6000 ng/ml	28
RP - HPLC	Reverse Phase High Performance Liquid Chromatography was used using a UV detector at 210 nm	40 - 200 μ g/mL	29
Electrochemical	Direct-current differential electrolytic potentiometry was used	0.1-10 mg	32
Potentiometry	Equivalent point is detected directly, potentiometrically or spectrophotometrically	0.5-5 mg	33
Our Method	Kinetic Spectrophotometric method based on ligand Substitution reaction	1.25 μ M	

Bioactive ruthenium complexes exhibit wide range applications as antiamebic, immunosuppressant, DNA binder, antifungal, antileukemic, antimetastatic, antitumor, and anticancer. [37-42] The metal catalyzed Hg(II) / Ag(I), cyanide substitution from cyano complexes of Fe(II) / Ru(II) by heterocyclic ligand containing nitrogen have been reported by several authors. [43-45] These reactions have also been successfully used for the micro level determination of employed catalyst and drugs / compounds that can bind strongly with catalyst. Organosulfur moieties form a strong complex with Hg(II), thereby decreasing the cyanide substitution to a considerable extent as the organosulfur compounds substantially inhibit the catalytic efficacy of Hg(II). This inhibitory feature of thio compounds (with sulfur as -S-, -SH and S-) can be used for its trace level quantification using kinetic spectrophotometric method. CCys also reduces the catalytic efficacy of Hg(II), thereby reducing the Hg(II) catalyzed rate of cyanide substitution with pyrazine from [Ru(CN)₆]⁴⁻.

More authentic result will be observed with the reaction in hand as the uncatalyzed reaction between pyrazine and $[\text{Ru}(\text{CN})_6]^{4-}$ was not noticed under the studied reaction condition. Because of the strong inhibitory action of carbocysteine (CCys) towards the catalytic efficacy of $\text{Hg}(\text{II})$, we conceived a simple, reproducible, and rapid kinetic spectrophotometric approach for the micro level quantification of CCys in distinct water samples down to $1.25 \times 10^{-6} \text{ mol dm}^{-3}$. The current system is also employed for the swift quantification of CCys in drug formulations with high reproducibility and good accuracy.

2. RESULTS AND DISCUSSION

Numerous methods are available for the quantification of CCys [23-33]. The major drawbacks of these existing methods include complex methodology, high initial investment, time-consuming process, heavy equipment, and high cost of sample analysis. The problems such as complex methodology, high initial investment, time-consuming process, and heavy equipment for the quantification of CCys are solved by the proposed kinetic method. The method requires affordable chemicals and a visible spectrophotometer, making it cost effective. The determination of CCys by the developed method is simple, fast and highly reproducible.

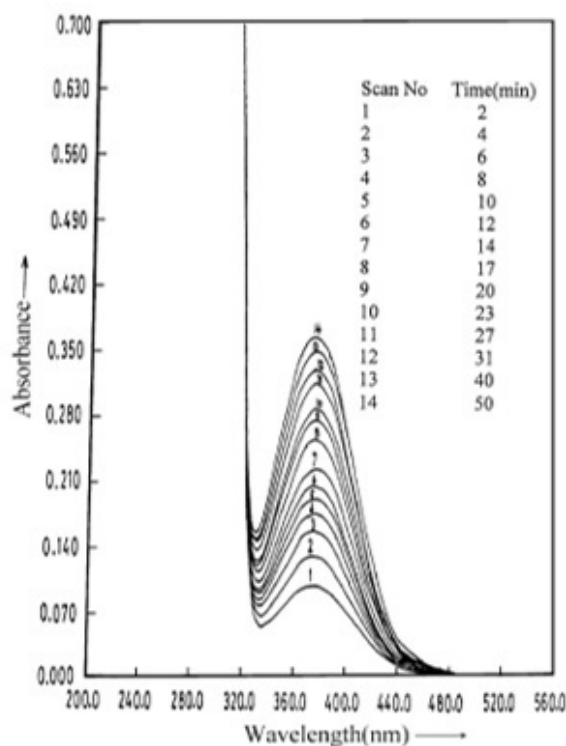


Figure 2: Repetitive spectral scan of a typical kinetic run at

$[\text{Ru}(\text{CN})_6]^{4-} = 2.75 \times 10^{-5} \text{ mol dm}^{-3}$, $I = 0.1 \text{ mol dm}^{-3}(\text{KCl})$, Temperature = $45.0 \pm 0.1^\circ \text{C}$, $[\text{Hg}^{+2}] = 1.5 \times 10^{-4} \text{ mol dm}^{-3}$, $[\text{Pyrazine}] = 3.0 \times 10^{-4} \text{ mol dm}^{-3}$, and $\text{pH} = 4.0 \pm 0.02$

The ultimate substitution product, $[\text{Ru}(\text{CN})_5 \text{Pz}]^{3-}$ is formed by the $\text{Hg}(\text{II})$ promoted reaction between pyrazine and $[\text{Ru}(\text{CN})_6]^{4-}$. During the reaction pyrazine and $[\text{Ru}(\text{CN})_6]^{4-}$ reacts in 1:1 mole ratio that was assured by mole ratio and slope ratio examination of ultimate reaction product. Since the all reacting solutions except the final reaction product exhibit no appreciable absorption at the studied wavelength, no correction in the absorption values were applied.^[45] The strong absorption band at 370 nm (Figure 2) belongs to the final product $[\text{Ru}(\text{CN})_5 \text{Pz}]^{3-}$ and is due to the metal to ligand charge transfer (MLCT) complex.

The preceding literature on D- penicillamine, thioglycolic acid, sodium thiosulphate, methionine, and carbocysteine admit that the sulfur compounds reduces the rate of $\text{Hg}(\text{II})$ catalyzed reaction between nitrogen donor ligand and $[\text{Ru}(\text{CN})_6]^{4-}$.^[34-36, 46-47] The observed reduced rate is due to the formation of stable complex by added sulfur compounds with $\text{Hg}(\text{II})$, which eventually reduces the active concentration of

Hg(II). CCys forms a stable complex with Hg^{2+} and reduces the actual Hg^{2+} concentration and ultimately the rate of reaction between pyrazine and $[\text{Ru}(\text{CN})_6]^{4-}$ catalyzed by Hg^{2+} .

The absorbance (A_t), corresponding to the ultimate reaction product $[\text{Ru}(\text{CN})_5 \text{Pz}]^{3-}$, with varying $[\text{CCys}]$ was computed at fixed time (9 and 14 min after mixing of reactants). A plot (calibration curve) of absorbance versus $[\text{CCys}]$, found to be linear in 1.25×10^{-6} - $5.00 \times 10^{-5} \text{ mol dm}^{-3}$ concentration range of CCys, did the quantification of CCys (Figure 3). The regression line relating A_t and $[\text{CCys}]$ can be expressed as Equation 1 and 2.

$$A_9 = 0.126 - 2.02 \times 10^3 [\text{CCYS}] \quad (1)$$

$$A_{14} = 0.153 - 2.32 \times 10^3 [\text{CCYS}] \quad (2)$$

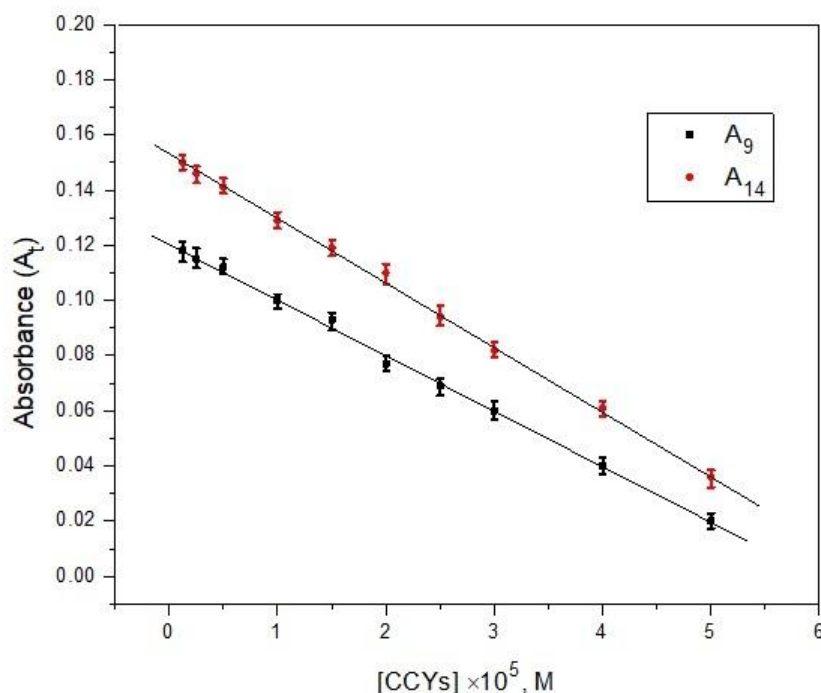


Figure 3: Calibration curve for quantification of Carbocysteine at $[\text{Ru}(\text{CN})_6^{4-}] = 2.75 \times 10^{-5} \text{ mol dm}^{-3}$, $I = 0.1 \text{ mol dm}^{-3} (\text{KCl})$, Temperature = $45.0 \pm 0.1^\circ \text{C}$, $[\text{Hg}^{+2}] = 1.5 \times 10^{-4} \text{ mol dm}^{-3}$, $[\text{Pyrazine}] = 3.0 \times 10^{-4} \text{ mol dm}^{-3}$, and $\text{pH} = 4.0 \pm 0.02$

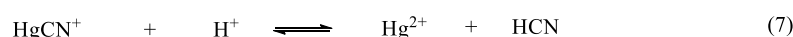
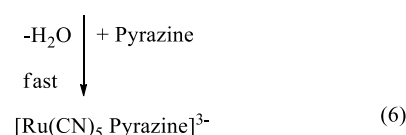
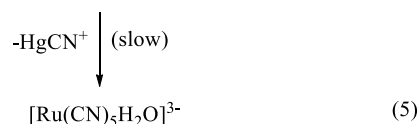
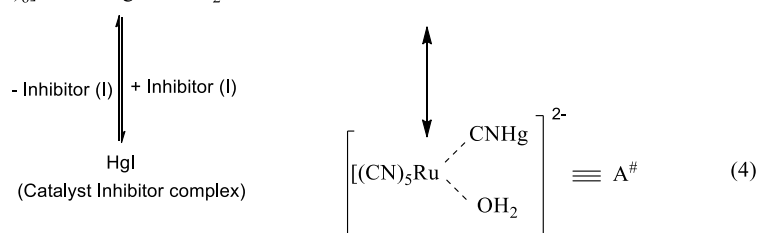
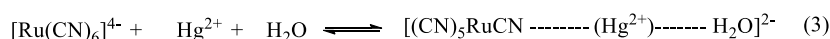
Table 2. Recovery results for CCys quantification

Reaction Condition: $[\text{Ru}(\text{CN})_6]^{4-} = 2.75 \times 10^{-5} \text{ mol dm}^{-3}$, $I = 0.1 \text{ mol dm}^{-3}$ (KCl), Temperature = $45.0 \pm 0.1^\circ \text{C}$, $[\text{Hg}^{2+}] = 1.5 \times 10^{-4} \text{ mol dm}^{-3}$, $[\text{Pyrazine}] = 3.0 \times 10^{-4} \text{ mol dm}^{-3}$, and pH = 4.0 ± 0.02

$[\text{CCys}] \times 10^5 \text{ mol dm}^{-3}$ (Taken)	A_9		A_{14}	
	$[\text{CCys}] \times 10^5 \text{ mol dm}^{-3}$ (Found)	Er ror	$[\text{CCys}] \times 10^5 \text{ mol dm}^{-3}$ (Found)	Erro r
0.35	0.36 ± 0.028	+	0.37 ± 0.046	+
0.45	0.45 ± 0.02	0.029	0.44 ± 0.05	-
0.75	0.77 ± 0.036	+	0.75 ± 0.00	0.022
1.05	1.03 ± 0.07	0.027	1.08 ± 0.042	0.00
1.30	1.30 ± 0.00	-	1.31 ± 0.06	+
1.55	1.56 ± 0.038	0.019	1.57 ± 0.03	+
2.05	2.02 ± 0.08	0.000	2.08 ± 0.068	0.029
2.55	2.57 ± 0.055	+	2.54 ± 0.042	+
		0.006		0.013
		-		+
		0.015		0.015
		+		-
		0.008		0.004

The calculated value of linear regression coefficient and standard error for A_9 and A_{14} plot (A_t versus $[\text{CCys}]$) was 0.9978, 0.9986 and 0.0014, 0.0015 respectively. To check the reproducibility and accuracy of the proposed kinetic method for CCys quantification, calculated amount of CCys was added to the reaction mixture and absorbance was noted at fixed time (9 and 14 min). Using calibration curve (Figure 3) the recovered CCys was computed and presented in Table 2. The recovered CCys data shows the reproducibility and accuracy of the proposed kinetic method.

The inhibitory action of CCys towards cyanide imitation from $[\text{Ru}(\text{CN})_6]^{4-}$ by pyrazine, catalyzed by Hg^{2+} has been demonstrated by a redesigned mechanistic scheme (Equations 3 – 7). More authentic result will be observed with the reaction in hand as the uncatalyzed reaction between pyrazine and $[\text{Ru}(\text{CN})_6]^{4-}$ was not noticed under the studied reaction condition.^[45]



Considering hexacyanoruthenate(II) as a single substrate with initial concentration S_o . In the presence of inhibitor (CCys), the catalyzed reaction rate can be deduced parallel to the enzyme-catalyzed reaction. Equation 8 represents the rate of catalyzed reaction (V_o) in the deflection of CCys.

$$V_o = \frac{V_{\max}}{1 + \frac{K_m}{[S_o]}} \quad (8)$$

Here K_m and V_{\max} give maximum rate at larger reactant concentration and Michaelis-Menten constant respectively. The straight line form ($1/V_o$ versus $1/[S_o]$) of the above equation having intercept and slope $1/V_{\max}$ and K_m/V_{\max} respectively and linear regression coefficient 0.9973, represented by Equation 9, is in accordance with Lineweaver-Burk expression.^[48]

$$\frac{1}{V_o} = \frac{1}{V_{\max}} + \frac{K_m}{V_{\max}} \frac{1}{[S_o]} \quad (9)$$

The K_m value calculated using slope and intercept of Figure 4 was 1.038 ± 0.014 mM.

The apparent M-M constant " K'_m ", in the inhibitor's presence, at constant catalyst concentration can be represented as:

$$K'_m = K_m \left(1 + \frac{[I_o]}{K'_{CI}} \right)$$

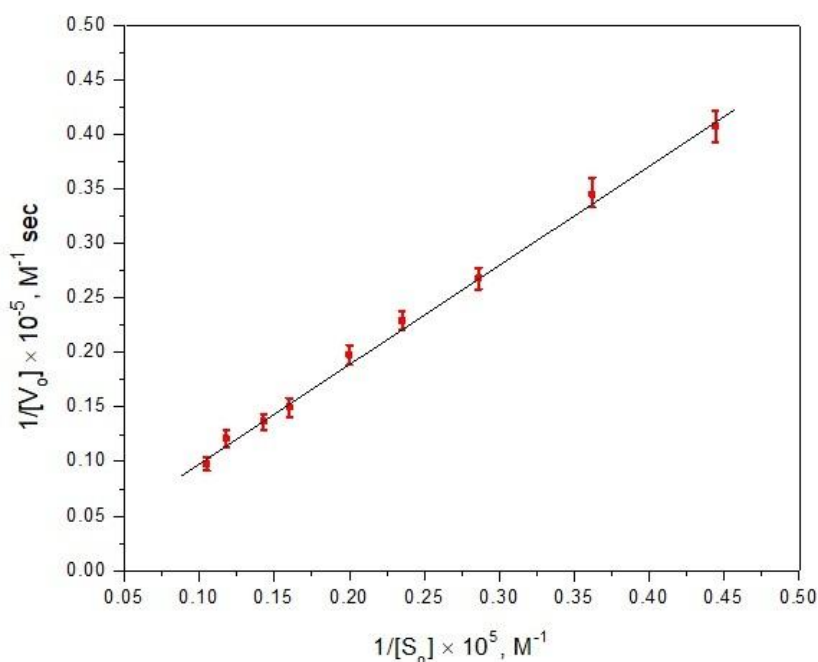


Figure 4: The Lineweaver-Burk plot at constant $[Hg^{+2}]$ in the absence of CCys at $I = 0.1 \text{ mol dm}^{-3}$ (KCl), Temperature = $45.0 \pm 0.1^\circ \text{C}$, $[Hg^{+2}] = 1.5 \times 10^{-4} \text{ mol dm}^{-3}$, $[Pyrazine] = 3.0 \times 10^{-4} \text{ mol dm}^{-3}$, and $pH = 4.0 \pm 0.02$

Where K'_{CI} corresponds to the catalyst-inhibitor complex's (C-I) dissociation constant while initial [CCys] is represented by I_o . The initial rate (V_i) in the inhibitor's presence, at constant catalyst concentration can be represented by Equation 10.^[49]

$$V_i = \frac{V_{\max}}{1 + \frac{K'_m}{[S_o]}} \quad (10)$$

$$V_i = \frac{V_{\max}}{1 + \frac{K_m}{[S_o]} \left(1 + \frac{[I_o]}{K'_{CI}}\right)} \quad (11)$$

The straight-line form of Equation 11 in accordance to Lineweaver-Burk equation can be given as Equation 12.

$$\frac{1}{V_i} - \frac{1}{V_{\max}} = \frac{K_m}{[S_o]V_{\max}} + \frac{K_m}{[S_o]V_{\max}} \frac{[I_o]}{K'_{CI}} \quad (12)$$

The intercept and slope of the linear plot between $\left(\frac{1}{V_i} - \frac{1}{V_{\max}}\right)$ and initial [CCys] (linear regression coefficient 0.9981) was used to determine the K'_{CI} and K_m (in the presence of CCys) value and were found to be $5.25 \times 10^{-5} \pm 0.06$ and 1.042 ± 0.012 mM respectively (Figure 5). The calculated K_m value in the presence and absence of CCys is almost same. The lower dissociation constant value ($5.25 \times 10^{-5} \pm 0.02$) suggests the highly stable nature of catalyst inhibitor complex.

2.1 Interference of co-existing components

Excipients, other than the active pharmaceutical ingredient are the inert compounds that are used as the vehicle, preservatives, coloring agents and fillers in pharmaceutical preparations. Optimized reaction conditions using the A_9 calibration curve, containing 1.0×10^{-5} mol dm⁻³ CCys and large number of distinct excipients was utilized to check the influence of excipients by performing recovery experiments. The recovery results show that the presence of maltitol, citrate, sodium lauril sulphate, and gelatin even up to 500 times to [CCys] do not exhibit any significant interference in CCys determination, while the CCys can be accurately determined in the presence of sorbitol, sucrose, magnesium stearate, lactose (up to 1000 times compared to CCys) by the proposed method (Table 3). The results demonstrate that by the developed method CCys can be accurately quantified even in the presence of the common additive present in drugs.

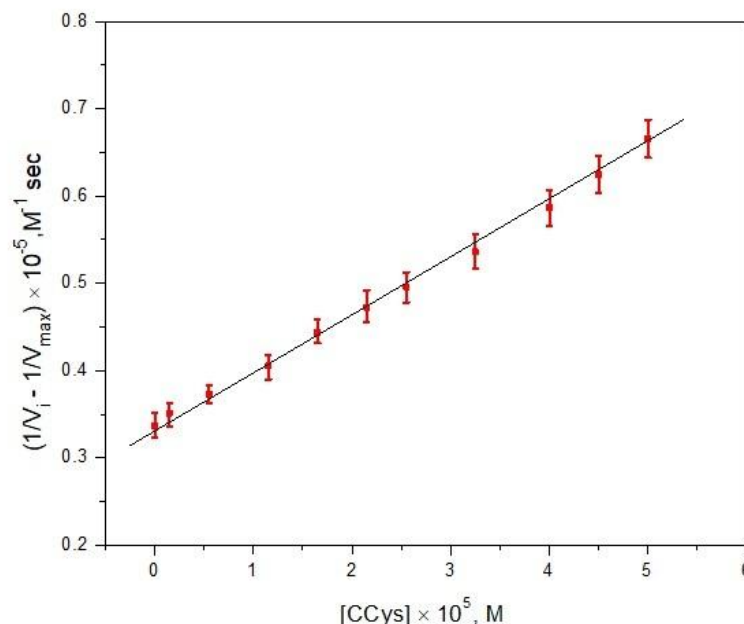


Figure 5: The plot of $(1/V_i - 1/V_{\max})$ versus initial [CCys] at $[Ru(CN)_6^{4-}] = 2.75 \times 10^{-5}$ mol dm⁻³, $I = 0.1$ mol dm⁻³ (KCl), Temperature = 45.0 ± 0.1 °C, $[Hg^{2+}] = 1.5 \times 10^{-4}$ mol dm⁻³, $[Pyrazine] = 3.0 \times 10^{-4}$ mol dm⁻³, and pH = 4.0 ± 0.02

Table 3. CCys Recovery results in the presence of excipients

Reaction Condition: $[\text{Ru}(\text{CN})_6^{4-}] = 2.75 \times 10^{-5} \text{ mol dm}^{-3}$, $I = 0.1 \text{ mol dm}^{-3}$ (KCl), Temperature = $45.0 \pm 0.1^\circ \text{C}$, $[\text{Hg}^{2+}] = 1.5 \times 10^{-4} \text{ mol dm}^{-3}$, [Pyrazine] = $3.0 \times 10^{-4} \text{ mol dm}^{-3}$, and pH = 4.0 ± 0.02

[CCys] $\times 10^5 \text{ mol dm}^{-3}$ (Taken)	Additives	[Additives] / [CCys]	[CCys] $\times 10^5 \text{ mol dm}^{-3}$ (Found)
1.0	Maltitol	500	0.993 \pm 0.007
1.0	Sorbitol	1000	0.996 \pm 0.005
1.0	Citrate	500	1.002 \pm 0.003
1.0	Sucrose	1000	1.003 \pm 0.004
1.0	Magnesium stearate	1000	1.008 \pm 0.006
1.0	Lactose	500	0.991 \pm 0.009
1.0	Sodium Lauril sulphate	1000	1.004 \pm 0.002
1.0	Gelatin	500	0.997 \pm 0.006

2.2 Application in pharmaceutical preparations

The quantitative determination of CCys in various drug samples was done by the suggested kinetic spectrophotometric method, for that the content of 10 tablet/capsule was weighed, ground, and dissolved in 100 ml of double distilled water. The solution thus obtained was sonicated for 20 min, after filtration via Whatman filter paper the concentration of various drug sampled were fixed to $1.5 \times 10^{-5} \text{ mol dm}^{-3}$. Five different drugs containing only CCys and excipients, obtained from local drug dealer were applied to the suggested kinetic method for the quantification of CCys. The obtained result is compared with the official method (Table 4).^[50] The statistical comparison and mean recovery (99-101 %) results demonstrate that with the proposed kinetic method CCys can be determined in distinct drug samples with good accuracy and reproducibility.

Table 4. CCys quantification in drug samples and comparison with the official method

Reaction Condition: $[\text{Ru}(\text{CN})_6^{4-}] = 2.75 \times 10^{-5} \text{ mol dm}^{-3}$, $I = 0.1 \text{ mol dm}^{-3}$ (KCl), Temperature = $45.0 \pm 0.1^\circ \text{C}$, $[\text{Hg}^{2+}] = 1.5 \times 10^{-4} \text{ mol dm}^{-3}$, [Pyrazine] = $3.0 \times 10^{-4} \text{ mol dm}^{-3}$, and pH = 4.0 ± 0.02

Drug Samples	[Drug] $\times 10^5 \text{ mol dm}^{-3}$ (Taken)	Recovery with Proposed Method \pm SD (%)	Recovery with Official Method \pm SD (%)
Mucodyne 375 mg Capsule (Elder Pharmaceuticals Pvt. Ltd.)	1.5	99.69 \pm 0.68	99.62 \pm 0.75
Mucosolv 375 mg Capsule (Cipla)	1.5	101.08 \pm 0.59	100.71 \pm 0.49
Loviscol 500 mg Capsule (Pfizer)	1.5	100.76 \pm 0.72	101.54 \pm 0.51
Flemaliz 500 mg Capsule (Flamingo Pharmaceuticals Pvt. Ltd.)	1.5	99.46 \pm 0.52	100.52 \pm 0.68
Mucoflem 500 mg Capsule (Centurion Laboratories)	1.5	99.94 \pm 0.73	98.94 \pm 0.38

3. METHOD VALIDATION

3.1 Accuracy

Recovery studies using standard addition method have been performed to access the accuracy of the proposed kinetic method. CCys recovery studies were performed with pure CCys (Table 2), in presence of excipients (Table 3), and in various drug formulations (Table 4). The recovered CCys demonstrates the accuracy of the proposed methodology.

3.2 Precision

The method precision was established by carrying out the analysis of homogenous aqueous solution obtained by dissolving tablets/capsules in water. The CCys quantification by the proposed analytical method was performed in five replicates. The values of relative standard deviation lie well within the limits indicated the sample repeatability of the method (Table 2, 3, and 4).

3.3 Limit of Detection (LOD) and Limit of Quantification (LOQ)

A plot of absorbance versus concentration of CCys was found to be linear in 1.25×10^{-6} - 5.00×10^{-5} mol dm^{-3} concentration range of CCys, with a coefficient of correlation, $r=0.9978$ for A_9 calibration curve. The regression line relating absorbance and [CCys] are given as Equation 1 and 2. The limit of detection and the limit of quantification were found to be 1.25×10^{-6} mol dm^{-3} and 3.5×10^{-6} mol dm^{-3} respectively.

4. CONCLUSION

A new fast, simple and well reproducible kinetic method was proposed for the quantitative determination of CCys based on the inhibitory property of the sulfur-containing compound CCys towards Hg(II). Since under the studied conditions pyrazine and hexacyanoruthenate(II) do not undergo chemical reaction in the absence of Hg(II), the studied reaction system provides more accurate results for the determination of CCys. The general additives present in pharmaceuticals do not significantly interfere with the determination of CCys, even if they are up to 1000 times the [CCys]. With the proposed kinetic spectrophotometric method, the quantification of CCys in various water samples can be performed at the micro level up to 1.25×10^{-6} mol dm^{-3} . The current system was also used for the rapid quantification of CCys in drug samples. The statistical comparison and mean recovery results (99-101%) demonstrate the reproducibility and accuracy of the proposed method for the quantification of CCys in water samples and drug formulations.

5. MATERIALS AND METHODS

5.1 Reagent Used

Analytical grade reagents and double deionized water was utilized through the whole kinetic study. To prevent the possible photo-degradation of pyrazine (99 % pure, Merck) and $\text{K}_4[\text{Ru}(\text{CN})_6] \cdot 3\text{H}_2\text{O}$ (99.95 % pure, Sigma-Aldrich), their stock solution were kept in amber colored bottles. Carbocysteine (> 98 % pure) was purchased from Sigma-Aldrich and was used as supplied. HgCl_2 (99 % pure, Merck) solution was prepared daily as it may be adsorbed on glass surface. Potassium hydrogen phthalate (99 % pure, Himedia) and HCl / NaOH (99 % pure, CDH Fine Chemicals) was applied to control the pH of the reaction medium while to regulate ionic strength of the reaction mixture KCl (99 % pure, Merck) was used.

5.2 Instrumentation and kinetic procedure

The pH of the reacting solutions was checked by Oakton digital benchtop pH meter model WW-35419-10, calibrated with predefined buffer solution. To record the absorbance at 370 nm corresponding to the ultimate reaction product $[\text{Ru}(\text{CN})_5 \text{Pz}]^{3-}$, A51119500C Multiskan Sky High Microplate Spectrophotometer

(ThermoFisher Scientific) was used. Since the all reacting solutions except the final reaction product do not exhibit appreciable absorption at the studied wavelength, no correction in the absorption values were applied. From the detailed, kinetic study of the reaction, an ideal reaction condition was judiciously selected that exhibit significant absorption change at 370 nm.^[45] After thermal equilibration (for 30 min at 45 °C) of all the reacting solution viz., $[\text{Ru}(\text{CN})_6^{4-}] = 2.75 \times 10^{-5} \text{ mol dm}^{-3}$, $\text{KCl} = 0.1 \text{ mol dm}^{-3}$, $[\text{Hg}^{2+}] = 1.5 \times 10^{-4} \text{ mol dm}^{-3}$, $[\text{Pyrazine}] = 3.0 \times 10^{-4} \text{ mol dm}^{-3}$, buffer of $\text{pH} = 4.0 \pm 0.02$, and CCys they are mixed promptly in the order: Pyrazine, HgCl_2 , buffer solution, KCl, CCys, and $[\text{Ru}(\text{CN})_6^{4-}]$. After brisk shaking, the reacting solution was promptly transported to the temperature controlled spectrophotometric cell. The temperature of the cell compartment was managed by self-designed circulating water arrangement system. The surge in absorbance corresponding to the ultimate product was recorded at fixed time. A plot (calibration curve) of absorbance versus varying [CCys] did the quantification of CCys.

Author contributions: Concept – Concept – A.S., N.S.; Design – A.S., N.S., R.S.; M.D.; Supervision – A.S.; Resources – A.S., N.S.; Materials – R.S.; M.D.; Data Collection and/or Processing – R.S.; M.D.; N.S.; Analysis and/or Interpretation – A.S., N.S., R.S.; M.D.; Literature Search – A.S., N.S., R.S.; M.D.; Writing – A.S., N.S.; Critical Reviews – A.S., N.S., R.S.; M.D.

Conflict of interest statement: None of the authors has any potential or actual conflict of interest to disclose in relation to the published article.

REFERENCES

- [1] Scaglione F, Petrini O. Mucoactive Agents in the Therapy of Upper Respiratory Airways Infections: Fair to Describe Them Just as Mucoactive? *Clin Med Insights Ear Nose Throat*. 2019; 12: 1179550618821930. [\[CrossRef\]](#)
- [2] Yasuda H, Yamaya M, Sasaki T, Inoue D, Nakayama K, Tomita N, Yoshida M, Sasaki H. Carbocysteine reduces frequency of common colds and exacerbations in patients with chronic obstructive pulmonary disease. *J Am Geriatrics Soc*. 2006; 54(2): 378–380. [\[CrossRef\]](#)
- [3] Hooper C, Calvert J. The role for S-carboxymethylcysteine (carbocysteine) in the management of chronic obstructive pulmonary disease. *Int J Chron Obstruct Pulmon Dis* 2008; 3(4): 659–669.
- [4] Rahman I. Pharmacological antioxidant strategies as therapeutic interventions for COPD. *Biochimica et Biophysica Acta (BBA) - Molecular Basis of Disease*. 2012; 1822(5): 714–728. [\[CrossRef\]](#)
- [5] Macciò A, Madeddu C, Panzone F, Mantovani G. Carbocysteine: clinical experience and new perspectives in the treatment of chronic inflammatory diseases. *Expert Opin Pharmacother*. 2009; 10(4): 693–703. [\[CrossRef\]](#)
- [6] Zeng Z, Yang D, Huang X, Xiao Z. Effect of carbocysteine on patients with COPD: a systematic review and meta-analysis. *Int J Chron Obstruct Pulmon Dis*. 2017; 12: 2277–2283. [\[CrossRef\]](#)
- [7] Drauz K, Grayson I, Kleemann A, Krimmer HP, Leuchtenberger W, Weckbecker C. "Amino Acids". *Ullmann's Encyclopedia of Industrial Chemistry*. Weinheim: Wiley-VCH. 2007. [\[CrossRef\]](#)
- [8] Tang K. Chemical diversity and biochemical transformation of biogenic organic sulfur in the ocean. *Front Mar Sci*. 2020; 7: 68. [\[CrossRef\]](#)
- [9] Abadie C, Tcherkez G. Plant sulphur metabolism is stimulated by photorespiration. *Commun Biol*. 2019; 2: 379. [\[CrossRef\]](#)
- [10] Kolluru GK, Shen X, Kevil CG. Reactive sulfur species: a new redox player in cardiovascular pathophysiology. *Arterioscler Thromb Vasc Biol*. 2020; 40: 874–884. [\[CrossRef\]](#)
- [11] Fukuto JM, Ignarro LJ, Nagy P, Wink DA, Kevil CG, Feelisch M, Cortese-Krott MM, Bianco CL, Kumagai Y, Hobbs AJ. Biological hydropersulfides and related polysulfides—a new concept and perspective in redox biology. *FEBS Lett*. 2018; 592: 2140–2152. [\[CrossRef\]](#)
- [12] Omondi RO, Stephen O, Ojwach SO, Jaganyi D. Review of comparative studies of cytotoxic activities of Pt(II), Pd(II), Ru(II)/(III) and Au(III) complexes, their kinetics of ligand substitution reactions and DNA/BSA interactions. *Inorg Chim Acta* 2020; 512: 119883. [\[CrossRef\]](#)
- [13] Naik RM, Srivastava A, Asthana A. The kinetics and mechanism of oxidation of hexacyanoferrate(II) by periodate ion in highly alkaline aqueous medium. *J Iran Chem Soc*. 2008; 5: 29–36. [\[CrossRef\]](#)
- [14] Iioka T, Takahashi S, Yoshida Y, Matsumura Y, Hiraoka S, Sato H. A kinetics study of ligand substitution reaction on dinuclear platinum complexes: Stochastic versus deterministic approach. *J Comput Chem*. 2019; 40: 279–285. [\[CrossRef\]](#)
- [15] Naik RM, Srivastava A, Verma AK, Yadav SBS, Singh R, Prasad S. The kinetics and mechanism of oxidation of triethylenetetraaminehexaacetate. *Bioinorg Reac Mech*. 2007; 6: 185–192. [\[CrossRef\]](#)

- [16] Srivastava A, Sharma V, Prajapati A, Srivastava N, Naik RM. Spectrophotometric determination of ruthenium utilizing its catalytic activity on oxidation of hexacyano ferrate(II) by periodate ion in water samples. *Chem Chem Technol.* 2019; 13(3): 275-279. [\[CrossRef\]](#)
- [17] Prasad S, Naik RM, Srivastava A. Application of ruthenium (III) catalyzed oxidation of Tris(2-amino ethyl) amine in trace determination of ruthenium in environmental water samples, *Spectrochim Acta A.* 2008; 70: 958-965. [\[CrossRef\]](#)
- [18] Rastogi R, Srivastava A, Naik RM. Kinetic and mechanistic analysis of ligand substitution of aquapentacyanoruthenate(II) in micelle medium by nitrogen donor heterocyclic ligand. *J Disp Sci Tech.* 2020; 41(7): 1045-1050. [\[CrossRef\]](#)
- [19] Srivastava A, Naik RM, Rastogi R. Spectrophotometric kinetic study of mercury(II) catalyzed formation of [4-CN-PyRu(CN)₅]³⁻ via ligand exchange reaction of hexacyanoruthenate(II) with 4-cyanopyridine – a mechanistic approach. *J Iran Chem Soc.* 2020; 17(9): 2327-2333. [\[CrossRef\]](#)
- [20] Huang Y, Lin T, Hou L, Ye F, Zhao S. Colorimetric detection of thioglycolic acid based on the enhanced Fe³⁺ ions Fenton reaction. *Microchem J.* 2019; 144: 190-194. [\[CrossRef\]](#)
- [21] Dedov AG, Marchenko DY, Zrelova LV. New method for determination of total of organic sulfur compounds in hydrocarbon media. *Pet Chem.* 2018; 58: 714-720. [\[CrossRef\]](#)
- [22] Kostara A, Tsogas GZ, Vlessidis AG, Giokas DL. Generic assay of sulfur-containing compounds based on kinetics inhibition of gold nanoparticle photochemical growth. *ACS Omega* 2018; 3(12): 16831-16838. [\[CrossRef\]](#)
- [23] Kyriacou D. Rapid voltammetric determination of methionine with a platinum electrode. *Nature* 1966; 211: 519-521. [\[CrossRef\]](#)
- [24] Nugrahani I, Abotbina IM, Apsari CN, Kartavinata TG, Sukranso Oktaviary R. Spectrofluorometric determination of L-tryptophan in canary (*Canarium indicum* L.) seed protein hydrolysate. *Biointerface Res Appl Chem.* 2019; 10(1): 4780-4785. [\[CrossRef\]](#)
- [25] Feng G, Sun S, Wang M, Zhao Q, Liu L, Hashi Y, Jia R. Determination of four volatile organic sulfur compounds by automated headspace technique coupled with gas chromatography–mass spectrometry. *J Water Supply Res T.* 2018; 67(5): 498-505. [\[CrossRef\]](#)
- [26] Mohamed W, El-Brashy A, Mohammed M, Amina A. Fluorimetric determination of carbocysteine and ethionamide in drug formulation. *Acta Chim Slov.* 2004; 51: 283-291.
- [27] Dhanure S, Savalia A, More P, Shirode P, Kapse K, Shah V. Bioanalytical Method for Carbocysteine in Human Plasma by Using LC-MS/MS: A Pharmacokinetic Application. *Sci Pharm.* 2014; 82(4): 765-776. [\[CrossRef\]](#)
- [28] Megoulas NC, Koupparis MA. Ion-chromatographic determination of carbocysteine in pharmaceuticals based on non-suppressed conductimetric detection. *J Chromatogr A.* 2004; 1026(1-2): 167-174. [\[CrossRef\]](#)
- [29] Argekar AP, Raj SV, Kapadia SU. Simultaneous determination of cephalixin and carbocysteine from capsules by reverse phase high performance liquid chromatography (RP - HPLC). *Anal Lett.* 1997; 30:4, 821-831. [\[CrossRef\]](#)
- [30] Chao Q, Sheng H, Cheng X, Ren T. Determination of sulfur compounds in hydrotreated transformer base oil by potentiometric titration. *Ana Sci.* 2005; 21: 721-724. [\[CrossRef\]](#)
- [31] Agrawal GP, Maheshwari RK, Mishra P. Validation of ultra-performance liquid chromatography-tandem mass spectrometry coupled with electrospray ionization method for quantitative determination of ornidazole in solid dispersion. *Curr Pharm Anal* 2020; 16(5): 487-493. [\[CrossRef\]](#)
- [32] Okawa A, Hayashi M, Inagaki J, Okajima T, Tamura T, Inagaki K. Novel method for L-methionine determination using L-methionine decarboxylase and application of the enzyme for L-homocysteine determination. *Biosci Biotechnol Biochem* 2020; 84: 927-935. [\[CrossRef\]](#)
- [33] El-Brashy AM, Al-Ghannam SM. Titrimetric determinations of some amino acids. *Microchemical J.* 1996; 53: 420-427. [\[CrossRef\]](#)
- [34] Srivastava A. Micro-level estimation of Mercaptoacetic acid using its inhibitory effect to mercury catalyzed ligand exchange reaction of hexacyanoruthenate(II). *Biointerface Res Appl Chem.* 2020; 10(6): 7152-7161. [\[CrossRef\]](#)
- [35] Agarwal A, Prasad S, Naik RM. Inhibitory kinetic spectrophotometric method for the quantitative estimation of D-penicillamine at micro levels. *Microchem J.* 2016; 128: 181-186. [\[CrossRef\]](#)
- [36] Srivastava A. Micro-level Estimation of Methionine Using Inhibitory Kinetic Spectrophotometric Method. *Biointerface Res Appl Chem.* 2021; 11(3): 10654-10663. [\[CrossRef\]](#)
- [37] Athar F, Husain K, Abid M, Azam A. Synthesis and anti-amoebic activity of gold(I), ruthenium(II), and copper(II) complexes of metronidazole. *Chem Biodiversity.* 2005; 2: 1320-1330. [\[CrossRef\]](#)
- [38] Bastos CM, Gordon KA, Ocain TD. Synthesis and immunosuppressive activity of ruthenium complexes. *Bioorg Med Chem Lett.* 1998; 8: 147-150. [\[CrossRef\]](#)
- [39] Yu B, Rees TW, Liang J, Jin C, Chen Y, Ji L, Chao H. DNA interaction of ruthenium(II) complexes with imidazo [4,5-f] [1,10] phenanthroline derivatives. *Dalton Trans.* 2019; 48: 3914-3921. [\[CrossRef\]](#)
- [40] Gomes-Junior FA, Silva RS, Lima RG, Vannier-Santos MA. Antifungal mechanism of [RuIII(NH₃)₄catechol]⁺ complex on fluconazole-resistant *Candida tropicalis*. *FEMS Microbio Lett.* 2017; 364(9). [\[CrossRef\]](#)
- [41] Kenny RG, Marmion CJ. Toward multi-targeted platinum and ruthenium drugs – A new paradigm in cancer drug treatment regimens? *Chem Rev.* 2019; 119: 1058-1137. [\[CrossRef\]](#)
- [42] Gu L, Lia X, Ran Q, Kang C, Lee C, Shen J. Antimetastatic activity of novel ruthenium (III) pyridine complexes. *Cancer Med.* 2016; 5: 2850-2860. [\[CrossRef\]](#)

- [43] Naik RM, Tewari RK, Singh P, Tiwari AK, Prasad S. The mercury(II) catalyzed ligand exchange between hexacyanoferrate(II) and pyrazine in aqueous medium. *Trans Met Chem* 2005; 30(8): 968-977. [\[CrossRef\]](#)
- [44] Naik RM, Chaturvedi DD, Srivastava A, Verma AK, Tiwari AK, Agarwal A. The Kinetics and mechanism of acid assisted reduction of unsymmetrical chelate complex $[\text{CoIII}(\text{Am})\text{endibig H}(\text{ClO}_4)_2]$ where Am= amino acid and endibig H = ethylenedibiguanide. *Ind J Chem A* 2004; 43: 2105-2108.
- [45] Naik RM, Verma AK, Agarwal A. Kinetic and mechanistic study of the mercury(II)-catalyzed substitution of cyanide in hexacyanoruthenate(II) by pyrazine. *Trans Met Chem*. 2009; 34: 209-215. [\[CrossRef\]](#)
- [46] Srivastava A, Sharma V, Singh VK, Srivastava K. A Simple and Sensitive Inhibitory Kinetic Method for the Carbocysteine Determination. *J Mex Chem Soc*. 2022; 66: 57-69. [\[CrossRef\]](#)
- [47] Srivastava A. Quantitative estimation of D-Penicillamine in pure and pharmaceutical samples using inhibitory kinetic spectrophotometric method. *Biointerface Res Appl Chem*. 2021; 11(4): 11404-11417. [\[CrossRef\]](#)
- [48] Lineweaver H, Burk D. The determination of enzyme dissociation constants. *J Am Chem Soc*. 1934; 156: 658-666. [\[CrossRef\]](#)
- [49] Tinoco I, Sauer K, Wang JC. *Physical chemistry, Principles and applications in biological sciences*, Prentice-Hall Inc., New Jersey, USA, 1978, p. 351.
- [50] *British Pharmacopoeia*, Her Majesty's Stationary Office, London, 1995.